Electronic, transport, and magnetic properties of CaxCo4Sb12 partially filled skutterudites

M. Puyet, Bertrand Lenoir, A. Dauscher, P. Pécheur, C. Bellouard, J. Tobola, J. Hejtmanek

Electronic, transport, and magnetic properties of $Ca_xCo_4Sb_{12}$ partially filled skutterudites

M. Puyet, B. Lenoir,* A. Dauscher, and P. Pécheur
Laboratoire de Physique des Matériaux, UMR 7556, Ecole nationale Supérieure des Mines de Nancy, Parc de Saurupt, CS14234, 54042 Nancy Cedex, France

C. Bellouard
Laboratoire de Physique des Matériaux, UMR 7556, Université Henri Poincaré-Nancy I, BP 239, 54506 Vandoeuvre les Nancy Cedex, France

J. Tobola
Faculty of Physics and Applied Computer Science, AGH university of Science and Technology, 30-059 Krakow, Poland

J. Hejtmanek
Institute of Physics Academy of Sciences of the Czech Republic, Cukrovarnicka 10, CZ-162 53 Praha 6, Czech Republic
(Received 1 August 2005; published 27 January 2006)

The physical properties of partially filled $Ca_xCo_4Sb_{12}$ ($x=0.03$, 0.05, 0.10, and 0.20) skutterudites have been investigated at low temperature. Electrical, transport, and magnetic data completed by specific heat data are discussed in view of electronic structure Korringa-Kohn-Rostoker method with consistent potential approximation calculations. Unusual electron transport characteristics in $Ca_xCo_4Sb_{12}$—namely, a complex variation of resistivity curves whereas a rather systematic variation of thermopower with Ca content—seem to be governed by a remarkably large *s*-like density of states appearing at the conduction band. These features corroborate the large effective masses estimated from Hall and thermopower measurements. The evolution of the density of states near the Fermi level agrees with the sign and variation of the Seebeck coefficient slope α/T versus Ca content. The comparison between the values of the electronic specific heat of $Ca_{0.20}Co_4Sb_{12}$ and Co_4Sb_{12} apparently supports the finite density of states at E_F in $Ca_{0.20}Co_4Sb_{12}$. The analyses of the Pauli paramagnetic susceptibility and specific heat behaviors concerning the carrier effective mass are coherent both with the electron transport measurements and the electronic structure features.

DOI: 10.1103/PhysRevB.73.035126 PACS number(s): 71.20.Nr, 72.20.Pa, 75.20.Ck

I. INTRODUCTION

Among metals and narrow-band-gap semiconductors, skutterudites have received particular attention these last years. This is not only for their interest as engineering materials in thermoelectric devices operating above room temperature, but also because they present interesting physical features from a fundamental point of view.[1] In particular, some skutterudites exhibit superconductivity and long-range magnetic order as well as rather exotic electronic-state features.[2–4]

The essence of a good thermoelectric material is captured in the material's dimensionless figure of merit, *ZT*, defined by

$$ZT = \frac{\alpha^2}{\rho\lambda}T, \tag{1}$$

where α is the Seebeck coefficient or thermopower, T the absolute temperature, ρ the electrical resistivity, and λ the total thermal conductivity. High *ZT* values significantly contribute to achieve high-efficiency thermoelectric devices. The challenge lies then in achieving simultaneously high α, low ρ, and low λ for a given thermoelectric material at the operating temperature T. The three transport properties are linked to the details of the electronic structure and to the scattering of the charge carriers and are thus mutually not independent.

The name "skutterudite" refers to the class of materials with a general formula MX_3 where M is a transition metal such as Co, Rh, or Ir and X stands for a pnictogen atom such as P, As, or Sb. Skutterudites crystallize in the body-centered-cubic structure, space group $Im3$ (No. 204). The structural "filling" refers to the total or partial occupation of the two interstitial sites (void sites) of the structure with no change in space group. Thermoelectric properties can be optimized through such judicious filling of the skutterudite structure and/or by substitutions on the M or X sites. The filling of the voids with heavy "rattling" ions, which are weakly bonded to the lattice, is particularly promising because these ions exercise large local vibrations which disrupt the harmonic modes of the parent atoms.[1,5–27] In this context, tremendous effort has been made with the cobalt triantimonide $CoSb_3$ skutterudite and numerous atoms have been used to fill the voids of this structure.[8–18,21–27] If void filling was shown to effectively impede phonon transport, the introduction of an ion influences also drastically the electronic properties. The present study was prompted by recent results on $A_xCo_4Sb_{12}$ compounds partially filled with A=Ba (Refs. 15–17) and Ca (Refs. 24,25) exhibiting excellent thermoelectric properties at moderate temperature with $ZT \geqslant 1$ at $T=800$ K. While Ba and Ca are both alkaline-earth metals, their solubility limit differs significantly [$x=0.44$ Ba (Ref. 15) and $x=0.20$ Ca (Ref. 26)]. The influence of Ba and Ca on the transport properties in $A_xCo_4Sb_{12}$ skutterudites has been

TABLE I. Lattice parameter (a) (Ref. 26), relative density (d, defined as the ratio of the measured density to the theoretical density) (Ref. 26), carrier concentration (n,p), Hall mobility (μ_H), and reduced effective masses (m^*/m_0) measured at room temperature for the different $Ca_xCo_4Sb_{12}$ skutterudites studied.

Compound	a (nm)	d (%)	np, (cm^{-3})	μ_H ($cm^2/V\,s$)	m^*/m_0
$Co_4Sb_{12.24}$	0.90360	82	$p=2.5\times10^{18}$	598	
$Ca_{0.03}Co_4Sb_{12.44}$	0.90390	91	$n=3.7\times10^{19}$	31.2	1.4
$Ca_{0.05}Co_4Sb_{12.43}$	0.90423	83	$n=7.1\times10^{19}$	27.2	1.7
$Ca_{0.08}Co_4Sb_{12.45}$	0.90429	90	$n=3.2\times10^{20}$	5.5	3.2
$Ca_{0.20}Co_4Sb_{12.47}$	0.90498	92	$n=2.8\times10^{20}$	7.3	2.4

thoroughly discussed for temperatures $T>300$ K, but only little information is available at low temperatures where the basic physical phenomena are usually exacerbated.

In this paper, the low-temperature transport properties (including magnetotransport), magnetic properties, and specific heat have been explored in $Ca_xCo_4Sb_{12}$ ($x=0$, 0.03, 0.05, 0.08, 0.20) polycrystalline samples. To have a deeper insight into this material system, electronic structure calculations have been performed and compared to results obtained with other alkaline-earth metals as the filler ions. There was a two-fold purpose for these electronic structure calculations in $A_xCo_4Sb_{12}$ (A=Mg, Ca, Sr, Ba) skutterudites. First, we intended to study the variations of the density of states (DOS) in $Ca_xCo_4Sb_{12}$ versus Ca content to better understand the influence of Ca content on the measured electron transport properties. Second, the isoelectronic elements Mg, Ca, Sr, and Ba inserted into the $CoSb_3$ matrix have been also considered to get more insight into the DOS behaviors near the Fermi level. Note that the chemical synthesis and some physical properties are, to the best of our knowledge, only reported for $Ba_xCo_4Sb_{12}$ (Ref. 16), $Ca_xCo_4Sb_{12}$ (Refs. 24,26), and $Sr_xCo_4Sb_{12}$ (Ref. 27) partially filled skutterudites; thus, $Mg_xCo_4Sb_{12}$ remains hypothetical. Nevertheless, comparing electronic structures of $A_xCo_4Sb_{12}$ in a systematic way along the alkaline-earth metal series allows us to elucidate some general trends and to underline rather unique electronic properties of the Ca partially filled $CoSb_3$ skutterudites.

II. EXPERIMENTAL AND COMPUTATIONAL DETAILS

Polycrystalline samples of $Ca_xCo_4Sb_{12}$ with $x\leqslant0.2$ were prepared by solid-state reactions.[26] High-purity Ca pellets (99.5%), Co powders (99.999%), and Sb shots (99.999%) were used as the starting materials. Stoichiometric amounts of these elements were loaded into a quartz ampoule in an argon-atmosphere glove box. The ampoule was heated up to 750 °C at a rate of 1 °C/min and left at 750 °C for 84 h. The obtained solid was then ground in an agate mortar into fine powders (<100 μm) that were further compacted into pellets. To achieve completely the reaction and to obtain the expected crystallographic phase, the tablets were annealed at 620 °C for 84 h. These materials were powdered again and densified. The densification was accomplished by hot pressing using graphite dies in an argon atmosphere at 600 °C for 2 h under 660 kg/cm^2.

Structural and chemical characterizations of the polycrystalline samples were achieved through x-ray diffraction, neutron diffraction, and electron probe micro-analysis (EPMA). The details of the characterizations have been previously reported elsewhere.[26] The main results are summarized in Table I. All the compositions given in this table have been normalized to full occupancy of the cobalt site and correspond to the actual composition.

For the transport and magnetic studies, bar-shaped specimens were cut with a diamond wire saw from the densified pellets to final typical dimensions of $2\times2\times10$ mm^3. Four-probe electrical resistivity and steady-state thermoelectric power were performed from 10 to 300 K using an automated closed-cycle refrigerator system. Magnetotransport measurements, including magnetoresistance and Hall measurements, were performed with an ac transport measurement system option (physical property measurement system, PPMS-Quantum Design) over the temperature range of 2–350 K and under a magnetic field ranging up to 7 T. Ohmic contacts to the samples were made with fine copper wires attached with care using a tiny amount of silver paint. Magnetization curves were measured from 5 to 300 K under a magnetic field up to 7 T using a commercial superconducting quantum interference device magnetometer (magnetic property measurement system, MPMS-Quantum Design). Specific heat measurements were carried out between 5 and 150 K on some selected samples using a PPMS.

Electronic structure calculations of the above-mentioned compounds were performed using the Korringa-Kohn-Rostoker method with consistent potential approximation (KKR-CPA).[28,29] The crystal potential was constructed within the local density approximation (LDA) using the Barth-Hedin expression for the exchange-correlation potential. The radii of nonoverlapping muffin-tin spheres (r_{Co} =1.11 Å, r_{Sb}=1.41 Å, and r_A=1.93 Å) have been chosen to obtain optimal filling of the Wigner-Seitz cell. For final crystal potentials, the total and site- and l-decomposed (with $l_{max}=2$) DOS have been computed using a tetrahedron k-space integration technique. The CPA cycles have been carried out in the complex energy plane using the elliptic contour, and the Fermi level (E_F) has been determined precisely via the generalized Lloyd formula.[30] Bearing in mind that KKR-CPA calculations of electron transport coefficients (i.e., electrical conductivity and thermopower) require a much more elaborate treatment accounting for the electron velocity dependence on the k vector and then integrating

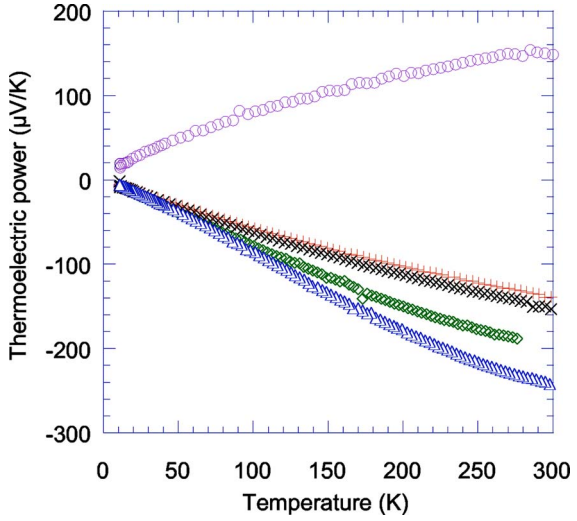

FIG. 1. (Color online) Temperature dependences of the thermoelectric power α for the $Ca_xCo_4Sb_{12}$ skutterudites, with (◯) $x=0$, (△) $x=0.03$, (◇) $x=0.05$, (×) $x=0.08$, and (+) $x=0.20$.

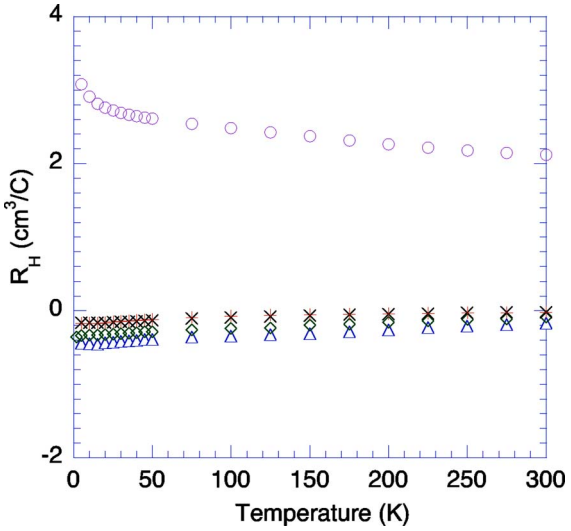

FIG. 2. (Color online) Temperature dependences of the Hall coefficient R_H for the $Ca_xCo_4Sb_{12}$ skutterudites, with (◯) $x=0$, (△) $x=0.03$, (◇) $x=0.05$, (×) $x=0.08$, and (+) $x=0.20$.

over the Fermi surface to obtain the transport function[31] (being a difficult task in such a complex disordered material), we have only performed a very rough analysis of the thermopower variations based on the computed KKR-CPA density of states in $Ca_xCo_4Sb_{12}$.

The experimental values of the structural parameters were employed in computations of $Ca_xCo_4Sb_{12}$. In the case of $A_xCo_4Sb_{12}$ (A=Mg, Ca, Sr, Ba and with x about 0.01), lattice constant (a=9.036 Å, Table I) and Sb positional parameters (u=0.3352, v=0.1578) (Ref. 26) of the binary $CoSb_3$ were used.

III. RESULTS AND DISCUSSION

A. Transport and magnetotransport properties

1. Thermopower and Hall concentration

The temperature dependence of the thermoelectric power has been measured between 4.2 and 300 K on the different $Ca_xCo_4Sb_{12}$ (x=0, 0.03, 0.05, 0.08, 0.20) skutterudites (Fig. 1). The $CoSb_3$ binary compound exhibits a positive thermoelectric power that increases with the enhancement of the temperature to attain a value close to 150 μV/K at room temperature. Such a behavior is typical of a diffusive thermoelectric power encountered in extrinsic semiconductors. No particular feature that could be attributed to phonon drag has been observed for temperatures lower than 50 K, as reported for single-crystalline $CoSb_3$.[8,32] The achievement of a p-type conduction is in good agreement with the results reported for instance by Nolas *et al.*[9] and Sharp *et al.*[5] on polycrystalline $CoSb_3$ samples. They however differ from those of Morelli *et al.*[8] and Kuznetsov *et al.*[22] in that they obtained a negative thermoelectric power in a similar temperature range. The origin of these discrepancies on the n or p type of conduction at low temperature in $CoSb_3$ skutterudites has been discussed by several authors. According to Morelli *et al.*,[8] the p- (n-) type behavior would be due to a lack of cobalt (antimony), respectively. These conclusions are partially supported by band structure calculations aiming to study the influence of defects on the density of states of the $CoSb_3$ compound.[33] It is, however, now well established that the purity of the raw cobalt material plays an essential role in the electrical properties encountered in $CoSb_3$.[34,35] The use of cobalt free of residual impurities of nickel (as is the case in this study) leads to a systematically positive thermoelectric power. Some hundreds of ppm of residual impurities of nickel in cobalt are enough to switch the material from p-type conduction towards n-type conduction.[36]

The introduction of calcium in the cavities of the skutterudite structure has a strong effect on the thermoelectric power behavior, as can be seen in Fig. 1. The presence of Ca at a content as low as x=0.03 leads to a negative thermoelectric power, indicating that the electrical conduction goes from a conduction dominated by the holes in $CoSb_3$ to a conduction dominated by the electrons in the $Ca_xCo_4Sb_{12}$ compounds. The thermoelectric power increases quasimonotonously with temperature in all the Ca containing skutterudites, a dependence that is typical of strongly doped semiconducting materials. The higher the calcium content is, the lower the thermoelectric power is. This suggests, in a first approximation, an increase of the charge carrier density with the increase of calcium content, the effect being more marked at higher temperatures. At room temperature, the value of the thermoelectric power varies between −250 and −140 μV/K for x =0.03 and 0.20, respectively. These high negative values are similar to those observed in $CoSb_{3-x}Te_x$ or $Co_{1-x}Pd_xSb_3$.[6]

In Fig. 2 are reported the temperature dependences of the Hall coefficient R_H for the different $Ca_xCo_4Sb_{12}$ samples. R_H is positive for the $CoSb_3$ binary compound, suggesting hole conduction, while it is negative in the Ca-containing compound, suggesting electronic conduction. These results therefore confirm those obtained from the thermoelectric power measurements. For all the Ca-containing samples, the R_H values are quasiconstant in the whole temperature range considered. Their smaller absolute value with regard to $CoSb_3$

could signify a higher density of electron-like charge carriers than that of hole-like carriers in $CoSb_3$.

If we assume the presence of one type of carriers only and a parabolic dispersion relation, the electron (hole) concentration n (p) can be estimated from the relation

$$n(p) = -(+)\frac{f}{R_H e}, \tag{2}$$

where e is the elementary charge and f the Hall factor. The Hall factor depends generally on the temperature, the scattering mechanisms of the charge carriers, and the Fermi level. For degenerate systems, f does not deviate from unity of more than 10%. This parameter was therefore assumed to be equal to 1, as has already been done by several other authors.[8,9,18,22,23] Note, however, that very recent *ab initio* full potential linear and augmented-plane-wave (FLAPW) calculations of the Hall coefficient in doped $CoSb_3$ skutterudites have revealed that the Hall factor changed from $f \approx 1.1$ for $n < 2.1 \times 10^{20}$ to $f \approx 1.6$ for $n > 2.7 \times 10^{20}$.[31]

The charge carrier densities calculated from Eq. (2) at $T = 300$ K increase with calcium content up to a value of $n = 3.2 \times 10^{20}$ cm^{-3} for $x = 0.08$. This high concentration seems to be a maximum (Table I) and stands typically for strongly doped semiconducting materials. It is nevertheless surprising that such values are encountered together with high values of the thermoelectric power. This fact could be associated with a high effective mass of the electrons, m^*, which can be estimated numerically by using a simple parabolic-band model and the experimental values of the thermoelectric power and carrier concentration measured at room temperature. If the most prominent scatters of charge carriers are the acoustic phonons (hypothesis that will be verified later on), the thermoelectric power and the electron concentration express as[37]

$$\alpha = -\frac{k_B}{e}\left(\frac{2F_1(\eta)}{F_0(\eta)} - \eta\right) \tag{3}$$

and

$$n = \frac{4}{\sqrt{\pi}}\left(\frac{2\pi m^* k_B T}{h^2}\right) F_{1/2}(\eta), \tag{4}$$

where F_i is the Fermi integral of order i, η the reduced Fermi level ($\eta = E_F/k_B T$), k_B the Boltzmann constant, and h the Planck constant. The electron effective mass is determined from the value of η calculated from Eq. (3) that is introduced in Eq. (4). The results indicate that the reduced effective mass m^*/m_0, where m_0 is the mass of the free electron, is relatively high in the $Ca_xCo_4Sb_{12}$ compounds, increasing from 1.4 for $x = 0.03$ to 3.2 for $x = 0.08$ (Table I). These values fit well with those found for other host atoms (Ce,[8] La,[9] Tl,[13] Ba,[15–17] Nd[22]). The relatively high values of m^*/m_0 are consistent with band structure calculations carried out on $CoSb_3$ for which a high effective mass was predicted for the conduction band.[33,38,39] Moreover, the m^*/m_0 values observed experimentally depend on n, suggesting a modification of the band structure consecutive to the presence of Ca host atoms.

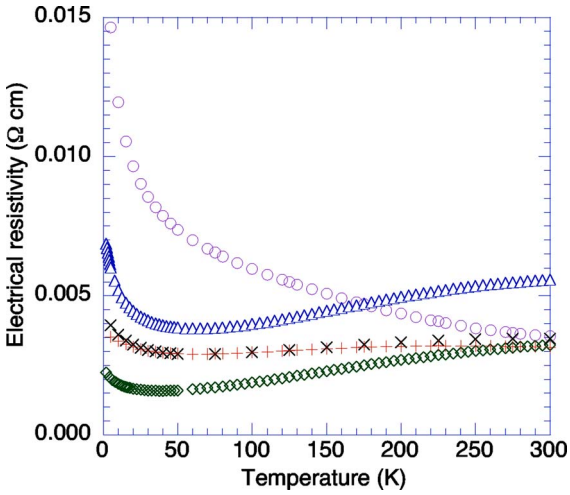

FIG. 3. (Color online) Temperature dependences of the electrical resistivity ρ for the $Ca_xCo_4Sb_{12}$ skutterudites, with (◯) $x = 0$, (△) $x = 0.03$, (◇) $x = 0.05$, (×) $x = 0.08$, and (+) $x = 0.20$. The values have not been corrected with regard to the porosity of the samples.

2. Electrical resistivity and Hall mobility

In Fig. 3 are reported the temperature dependences of the electrical resistivity ρ of the different skutterudites studied. The binary $CoSb_3$ compound exhibits an electrical resistivity that diminishes as a function of temperature, characteristic of a semiconducting behavior, although its carrier density is relatively high ($p \sim 2.5 \times 10^{18}$ cm^{-3}). These observations are in good agreement with results in the literature obtained for polycrystalline p-type $CoSb_3$.[5,9,40]

Calcium insertion in the cavities of the crystalline structure modifies somewhat the temperature dependence since the electrical resistivity decreases, exhibits a minimum, and then increases slowly when the temperature further increases. Moreover, the electrical resistivity does not diminish continuously with the quantity of inserted calcium as one could presume, but varies in a quite chaotic way. Such anomalies were not noticed with host atoms like Ce,[8] La,[9] or Nd.[22] It would have been interesting to compare with Ba, another alkaline-earth atom, but unfortunately, no data have been published for low temperatures except for the mobility.[16] The temperature at which the minimum of $\rho(T)$ appears depends on the Ca content, but *a priori* with no apparent tendency. Modeling of the electrical resistivity behavior has been attempted for temperatures lower than this resistivity minimum. An adjustment of the experimental results by a thermal activation law of type $\rho \sim e^{\Delta/T}$ revealed to be fruitless. However, the resistivity follows quite well a Mott law:[41]

$$\rho = \rho_0 \exp\left[\left(\frac{T_0}{T}\right)^{1/4}\right], \tag{5}$$

where ρ_0 and T_0 are two constants, as illustrated in Fig. 4. Equation (5) suggests a localization of the charge carriers supporting impurity-band conduction. Beyond the resistivity minimum, the electrical resistivity of the calcium partially filled skutterudites exhibits a metalliclike behavior. As mentioned above the Hall coefficient varies little in the tempera-

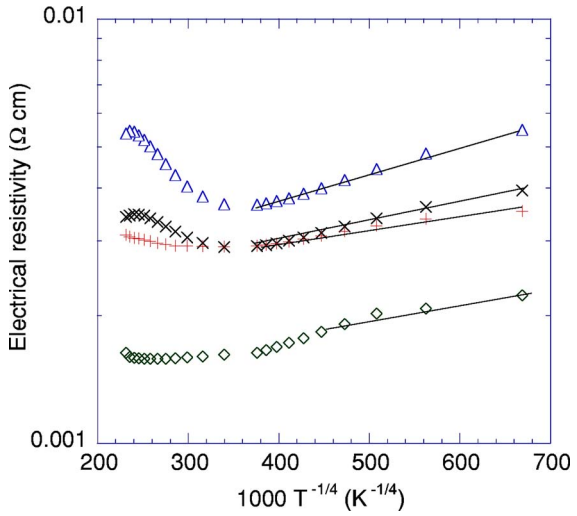

FIG. 4. (Color online) Electrical resistivity as a function of $T^{-1/4}$ for the $Ca_xCo_4Sb_{12}$ skutterudites, with (◯) $x=0$, (△) $x=0.03$, (◇) $x=0.05$, (×) $x=0.08$, and (+) $x=0.20$.

ture range considered and the increase of resistivity would simply reflect the decrease of the mobility of the charge carriers.

Although the carrier densities of the Ca containing compounds are one order of magnitude superior (or even more) to that of $CoSb_3$, the values of the electrical resistivity of these materials at room temperature are very close ($\sim 3 \times 10^{-3}$ Ω cm), except for the sample with $x=0.03$ (Fig. 3). These facts can be mainly explained by the differences in mobility of the two types of carriers, linked to differences in the effective masses of holes and electrons.

The Hall mobility μ_H is represented in Fig. 5 as a function of temperature. The values of μ_H at room temperature are given in Table I for all the studied materials. As one can predict, the *p*-type $CoSb_3$ shows a high value in comparison to the *n*-type materials at $T=300$ K. This value, close to 600 $cm^2/(V\,s)$, is nevertheless lower than those encountered

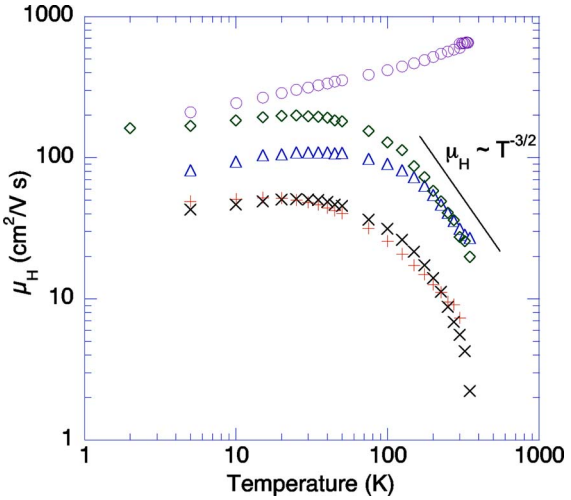

FIG. 5. (Color online) Temperature dependences of the Hall mobility μ_H for the $Ca_xCo_4Sb_{12}$ skutterudites, with (◯) $x=0$, (△) $x=0.03$, (◇) $x=0.05$, (×) $x=0.08$, and (+) $x=0.20$.

in *p*-type single crystals having similar carrier concentrations.[6] The *n*-type $Ca_xCo_4Sb_{12}$ materials possess a low mobility at $T=300$ K, generally decreasing when the calcium content increases. Considering similar filling fractions, Hall mobilities close to our values have been obtained with La partial filling.[9] However, the values are in general 3–5 times higher as, for instance, with Ce,[8] Tl,[13] Ba,[16] and Nd.[22]

Interesting information on the scattering mechanisms of the charge carriers can be deduced from the temperature dependences of the Hall mobility. For the *p*-type $CoSb_3$ compound (see Fig. 5), the Hall mobility increases with increasing temperature between 4 and 300 K. These results are in good agreement with those of the literature.[40,42] obtained on *p*-type polycrystalline samples exhibiting micron-sized grains, as is the case in our materials. We however exclude the possibility that the increase of mobility with temperature is linked to a scattering of holes at the grain boundaries because the temperature dependence does not follow the law $\mu_H \sim T^{-1/2} \exp[-E_B/k_BT]$ where E_B represents the activation energy characterizing the height of the barrier.[43] We rather think to a mixed scattering mechanism involving ionized impurities ($\mu_H \sim T^{3/2}$) as well as neutral impurities ($\mu_H \sim$ const).

For the *n*-type $Ca_xCo_4Sb_{12}$ samples, the mobility exhibits a behavior similar to that of $CoSb_3$ at low temperature for $x=0.03$ and $x=0.05$ while for $x=0.08$ and $x=0.20$, the dependences with temperature are weaker, suggesting than the mechanism dominating the scattering of the electrons is the scattering by the neutral impurities. Above 100 K, the mobility varies following a law close to $T^{-3/2}$, whatever the filling fraction is. This behavior is consistent with electron scattering by the acoustic phonons.

The behaviors of the temperature dependences of the Hall mobility taken between 4 and 300 K are close to those observed in skutterudites partially filled with Ba.[16] The only noticeable differences are the higher values for Ba-filled skutterudites that are 5 times enhanced at 300 K and more than one order of magnitude at 5 K.

Down to 5 K, the magnetoresistance of all the $Ca_xCo_4Sb_{12}$ compounds is positive whatever the magnetic field is. Moreover, the magnetoresistance varies in an almost linear manner with the square of the magnetic field, indicating a conventional behavior that can be attributed to the Lorentz strength.

B. Electronic structure

1. $A_xCo_4Sb_{12}$ (A=Mg, Ca, Sr, Ba)

The electronic structure of pure $CoSb_3$ was calculated using various band structure methods within the LDA framework.[31,33,38,39,44,45] It is well established that $CoSb_3$ is a narrow-band-gap semiconductor with the characteristic quasi linear behavior of one valence band.[38] It was also shown that the computed energy gap E_g strongly depends on the choice of the Sb positional parameters as well as on the lattice parameter, E_g varying from 0.07 eV to 0.22 eV in the different theoretical studies. The spin-orbit interactions appearing at the Γ point are quite weak [23 meV (Ref. 45)] in $CoSb_3$, and

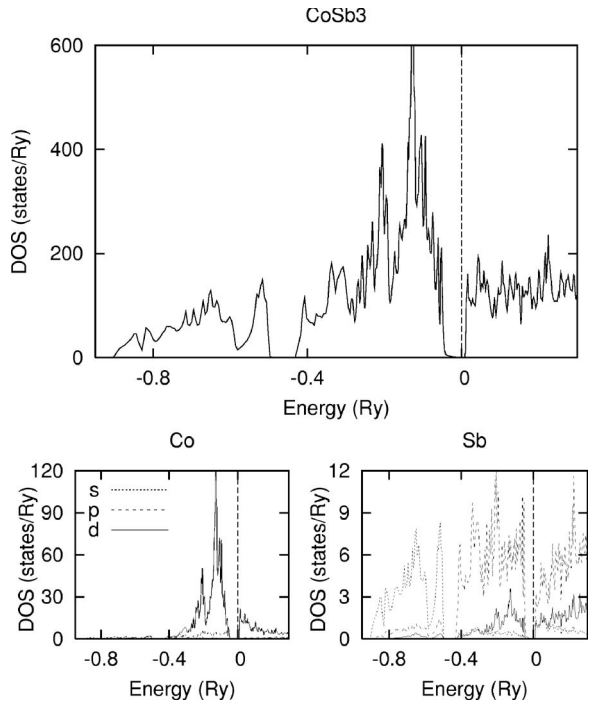

FIG. 6. Total (upper panel) and site-dependent (bottom panels) densities of states in $CoSb_3$. The Fermi energy is at zero (a vertical line) and *s*, *p* and *d* contributions to Co and Sb are plotted by dotted, dashed and solid lines, respectively.

they were neglected in the present KKR-CPA calculations (see Fig. 6). These KKR calculations confirm the semiconducting ground state of the binary $CoSb_3$ skutterudite.[7]

Our analysis starts from considering the electronic states of various elements *A* (Mg, Ca, Sr, Ba) in $A_xCo_4Sb_{12}$ ($x=0.01$). As we can see from the DOS plotted in Fig. 7, the self-consistent crystal potential is noticeably different for each element, despite the same number of valence electrons. For the light elements (Mg and Ca), the electronic states are dominated by the *s*-DOS which are confined in a sharp peak. This peak is located either inside the valley between the valence and conduction bands (Mg) or at the conduction band edge (Ca). For heavier elements (Sr and Ba), the *s* states are found inside the conduction band and form a broad peak due to the important hybridization with the host electronic structure (mainly *d*-Co states with admixture of *p*-Sb states). Especially in the case of Ba, the *s*-DOS is pushed up to the higher energy and the main contribution near the conduction band edge is attributed to *d*-symmetry states (found also below the energy gap). It is completely different from Ca-containing skutterudites for which the *s* states visibly dominate (Fig. 7). Noteworthy, the trend of the *s* states shifting towards higher energy with the increase of the total number of electrons *Z* along the alkaline-earth metal series is in line with the increase of the *ns* atomic energy level in the periodic table (the lowest energy of the $3s^2$ level in the Mg atom and the highest energy of $6s^2$ level in the Ba atom).

From the comparison of the electronic structures of the different $A_xCo_4Sb_{12}$ skutterudites, one can see that the Ca-DOS is rather uncommon to other *A* elements due to the presence of a large *s*-DOS peak at the conduction band edge. Indeed, this peculiar electronic structure behavior has an important effect on the electron transport properties, particularly at low temperatures.

2. $Ca_xCo_4Sb_{12}$

Figure 8 shows the total density of states in $Ca_xCo_4Sb_{12}$ for $x=0.02$, 0.05, 0.10, and 0.20. At a first glance, one notices that the total DOS strongly increases with Ca content. Comparing site-composed DOS on all atom sites (Fig. 8), the largest DOS value is found on calcium for intermediate concentrations ($x=0.05$ and 0.10), but this effect can be seen only a little on the total DOS (perhaps except for $x=0.05$) due to low Ca content. Inspecting the DOS on the Ca site (Fig. 9), one observes that at very low content (1%–2% Ca), the Fermi level is detected just below the large *s*-DOS peak from Ca and E_F starts to fall into this large peak for about $x=0.05$. The Fermi level resides inside this peak for higher *x* concentrations, but the *s* states begin to broaden due to the increasing hybridization with the conduction band states (mainly *d* states of Co). So in view of the KKR-CPA results, one can suggest that in the range of 5%–10% Ca content, the electrical conductivity should be essentially attributed to the filler carriers which are expected to have quite heavy electron masses (the Fermi level is located in the sharp Ca *s*-DOS). This is in qualitative agreement with the increase of the carrier masses from $1.4m_0$ for $x=0.03$ to $3.2m_0$ for $x=0.08$ and also with the carrier mobility maximum as observed experimentally in Fig. 5. In the same time, the DOS at E_F rapidly increases with *x* content, indicating a transition from a semiconducting-like to a more metallic-like state. This electronic structure behavior is also in line with the detected experimentally increase of the carrier concentration with Ca content. To support our suggestion of the conductivity mechanism (at least at 5%–10% Ca contents), the electron concentrations have been estimated assuming that the available electron carriers are only due to inserted Ca. Since the electronic structure calculations showed that each Ca

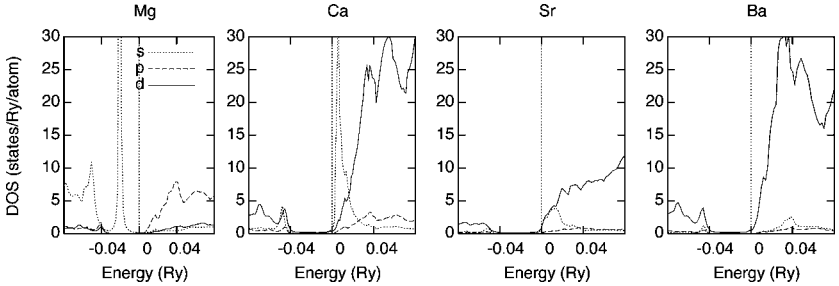

FIG. 7. Partial DOS of diluted alkaline-earth element *A* (*A*=Mg, Ca, Sr, Ba) in $A_xCo_4Sb_{12}$. The Fermi energy is at zero (a vertical line) and *s*, *p*, and *d* contributions are plotted by dotted, dashed, and solid lines, respectively.

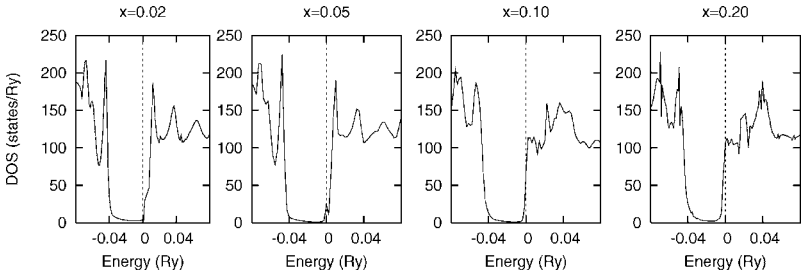

FIG. 8. Total DOS variation versus Ca content in $Ca_xCo_4Sb_{12}$ (x=0.02, 0.05, 0.10, 0.20). The Fermi energy is at zero (a vertical line).

atom acts as two electrons donors (essentially of s-like symmetry), the electron concentration $n=4.3\times10^{20}/\mathrm{cm}^3$ obtained for $x=0.08$ is in reasonable agreement with the measured value of $n=3.2\times10^{20}/\mathrm{cm}^3$. For higher Ca contents ($x=0.20$, Fig. 9), the DOS at E_F becomes more related to the electronic states of the host atoms (mainly d-Co) and the electrical conductivity seems to be driven by different channels. Following the DOS variation near E_F in $Ca_{0.20}Co_4Sb_{12}$, the conduction electrons are expected to possess lighter mass than in samples with $x=0.05$ and 0.08. This behavior seems to be supported by the experimental observations, since the refined effective mass again slightly decreases with Ca content increase (about $2.4m_0$ in $x=0.20$ sample versus $3.2m_0$ in $x=0.10$). On the other hand, it is not evident to explain from the KKR-CPA calculations the decrease of the carrier concentration observed from Hall measurements in both samples. In this case, the experimental carrier concentration should be corrected by the Hall factor expected to be different from unity.

Figure 10 presents the variation of the total and site-decomposed DOS at E_F versus Ca content. The KKR-CPA total density of states at the Fermi level, $N(E_F)$, is as large as 44.4, 67.5, and 98.8 states/Ry per $Ca_xCo_4Sb_{12}$ for $x=0.05$, 0.10, and 0.20, respectively (see the discussion of the specific heat data, Sec III D).

Let us try to roughly estimate the electron transport characteristics based on the calculated DOS in $Ca_xCo_4Sb_{12}$ compounds. The differential electrical conductivity $\sigma(E)$ can be regarded as proportional to the total density of states $N(E)$ and the carrier mobility $\mu(E)$—i.e., $\sigma(E)\sim N(E)\mu(E)$. Assuming that the carrier mobility $\mu(E)$ varies slowly with energy near the Fermi level, one can relate the variation of the electrical conductivity to the variation of $N(E)$ in the vicinity of E_F. Thermopower can be expanded in powers of temperature T:

$$\alpha(T) = AT + BT^3 + \cdots, \tag{6}$$

where the linear term denotes the contribution from the electron scattering (presumably dominating at low temperatures), whereas the second term represents the so-called "phonon-drag" contribution (expected to be small at low T in these samples; see above Sec. III A). Hence the coefficient $A=\alpha/T$ can be deduced employing the well-known Mott formula

$$\frac{\alpha}{T} = -\frac{\pi^2 k_B^2}{3e}\left(\frac{\partial \ln \sigma(E)}{\partial E}\right)_{E=E_F}. \tag{7}$$

In fact, as already mentioned, we look the DOS variation and then $\alpha/T=-\pi^2k_B^2/3e\ \mathrm{d}\ln N_{\mathrm{tot}}(E)/\mathrm{d}E$ at $E=E_F$. The sufficiently dense energy mesh in the vicinity of E_F has been used to allow for accurate numerical derivation of $\mathrm{d}\ln N_{\mathrm{tot}}(E)/\mathrm{d}E$. If $N_{\mathrm{tot}}(E)$ is the total density of states given in states/Ry, the α/T ratio in currently used units of thermopower ($\mu\mathrm{V/K}^2$) can be obtained from the relation $\alpha/T\ (\mu\mathrm{V/K}^2)=0.2877\times10^{-2}\ \mathrm{d}\ln N_{\mathrm{tot}}(E)/\mathrm{d}E\ (1/\mathrm{Ry})$. Numerical derivation of KKR-CPA DOS in $Ca_xCo_4Sb_{12}$ compounds yielded the following values of the α/T slope (in $\mu\mathrm{V/K}^2$): −1.14, −0.71, and −0.31 for $x=0.05$, 0.10, and 0.20, respectively. Bearing in mind that the thermopower values deduced from this simplified analysis should be taken with care (rather qualitatively than quantitively), the obtained theoretical values reflect quite well the trends observed from the low-temperature thermopower data. For example, at $T=100$ K, the computed values are (in $\mu\mathrm{V/K}$) −114, −71, and −31 versus the experimental data −74, −60, and −55, for $x=0.05$, 0.08, and 0.20 samples, respectively.

C. Magnetic properties

The magnetic behavior of the $Ca_xCo_4Sb_{12}$ skutterudites, which consists of nonmagnetic Ca, Co, and Sb atoms without local magnetic moments associated with unpaired valence electrons (Co is in the diamagnetic low spin state), should be controlled by a subtle balance between the temperature weakly dependent core and Langevin diamagnetism and Pauli and Van Vleck paramagnetism.[1,46] In this respect, and consistently with the calculated electronic structure we do

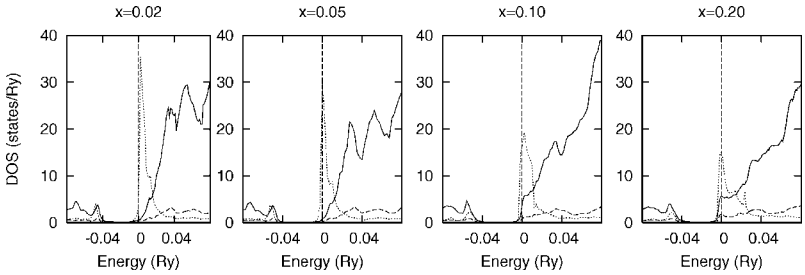

FIG. 9. Evolution of the partial DOS of Ca in $Ca_xCo_4Sb_{12}$ versus x concentration. The Fermi energy is at zero (a vertical line).

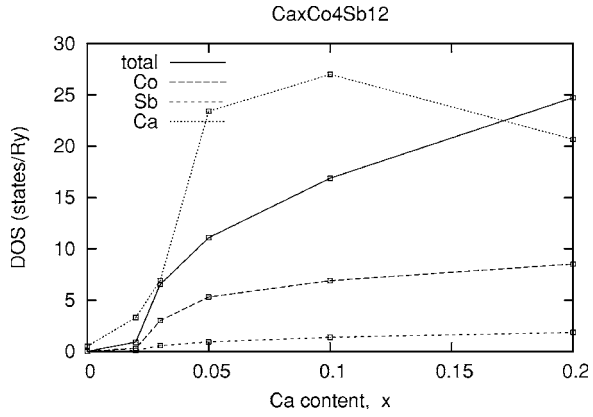

FIG. 10. Variation of the total and site-decomposed DOS at the Fermi level in $Ca_xCo_4Sb_{12}$ skutterudites.

not tend to associate the temperature-dependent Curie-Weiss paramagnetism, if observed, with local moment Co atoms in skutterudite lattice, as stipulated, e.g., by Chen *et al.* for $Ba_xCo_4Sb_{12}$.[15] Contrary to that, we propose to ascribe the Curie-Weiss paramagnetism to paramagnetic impurities, which are known to be difficult to eliminate during the skutterudite synthesis (for example, $CoSb_2$).[47]

In order to isolate the intrinsic susceptibility $\chi_{\text{intrinsic}}$ of the $Ca_xCo_4Sb_{12}$ phases from the raw magnetic data, we have measured and analyzed the isothermal magnetization curves for all the $Ca_xCo_4Sb_{12}$ samples, shown in Fig. 11. Here the most important task prior the analysis of $\chi_{\text{intrinsic}}$ is to subtract the "parasitic" magnetization arising from magnetic impurities. These can easily mask or even dominate the intrinsic magnetization, in particular ferromagnetic impurities at low magnetic fields and paramagnetic impurities of Curie character at low temperatures. Consequently, the magnetization data are analyzed by taking into account the (i) parasitic ferromagnetic component, which saturates at small fields, (ii) parasitic paramagnetic temperature-dependent Curie-Weiss component, evidenced by typical Brillouin magnetization curve at low temperatures, and, finally, (iii) "intrinsic" linear magnetization $M_{\text{intrinsic}}$ associated with $\chi_{\text{intrinsic}}$ with dominating diamagnetism. The small and temperature-independent ferromagnetic component differs for the different samples and is likely linked with parasitic ferromagnetic impurities. The paramagnetic component is more difficult to analyze and hence is exemplified separately in Fig. 12. The curves at 5 K were obtained by subtracting the diamagnetism and residual ferromagnetism at 300 K. Performing the Brillouin fit of the Curie-Weiss low-temperature magnetization curves, we were able to roughly estimate the concentration of the paramagnetic impurities. Supposing $CoSb_2$ as the most likely paramagnetic precipitates, their concentration in the prepared materials was found to vary between 60 and 850 ppm where the lowest is for $x=0.2$ and the highest for $x=0.08$. Similarly, considering the Co precipitates as ferromagnetic impurities, their concentration was estimated between 1 and 7 ppm with the lowest value for $x=0.08$ and the highest for $x=0.2$. After these corrections, we were able to isolate the mass intrinsic susceptibility at 300 K, which is together with other characteristics given in Table II.

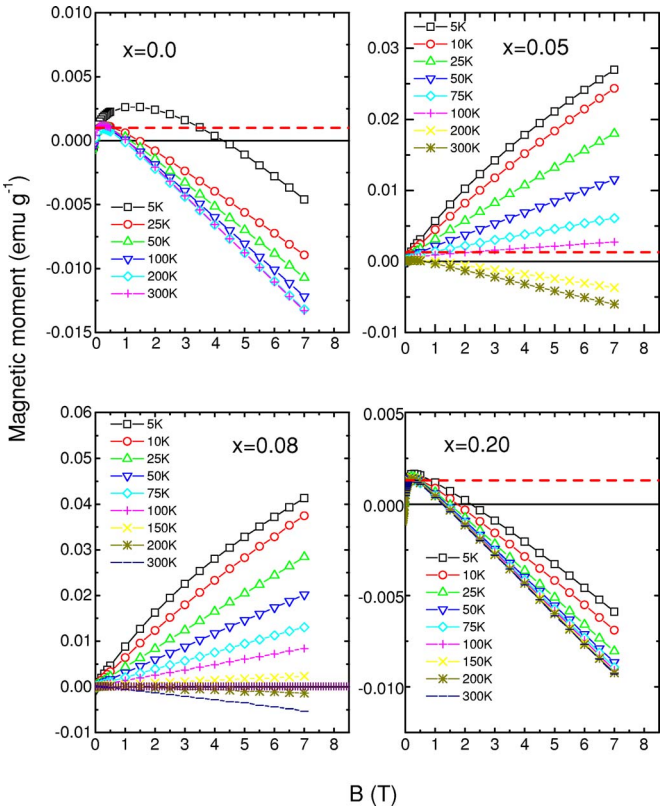

FIG. 11. (Color online) Magnetization data for $Ca_xCo_4Sb_{12}$ skutterudites. The extrapolated ferromagnetic impurity contributions at 300 K are represented by the dashed line.

The intrinsic $Ca_xCo_4Sb_{12}$ susceptibility can be further written using the formula

$$\chi_{\text{intrinsic}} = \chi_{\text{latt}} + \chi_{\text{Pauli}}. \tag{8}$$

The first term χ_{latt} is the lattice susceptibility, composed of core electron diamagnetism, Langevin-type diamagnetism of valence electrons, and a Van Vleck paramagnetic component reflecting the character of the chemical bond and asymmetry of the valence electrons. The second term χ_{Pauli} is the susceptibility of the charge carrier subsystem. With respect to the fact that skutterudites are studied due to their outstanding transport properties, the important task represents the evalu-

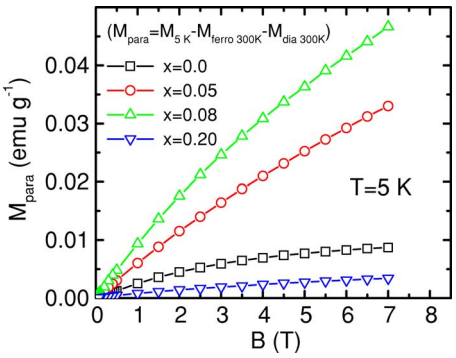

FIG. 12. (Color online) The Curie-Weiss paramagnetic contribution at 5 K for $Ca_xCo_4Sb_{12}$ skutterudites.

TABLE II. Magnetic and electronic properties of $Ca_xCo_4Sb_{12}$ skutterudites at 300 K. Susceptibilities $\chi_{intrinsic}$ and χ_{Pauli} are evaluated using experimental data; other characteristics are evaluated using electronic structure calculations.

Compound	$\chi_{intrinsic}$ (emu/g) $\times 10^{-7}$	$N(E_F)$ $\times$(states/Ry/mol)	χ_{LDA} (emu/mol) $\times 10^{-6}$	χ_{Pauli} (emu/mol) $\times 10^{-6}$	m^*/m_0
$Co_4Sb_{12.24}$	−2.24	0	0	68	
$Ca_{0.05}Co_4Sb_{12.43}$	−0.95	44	104	288	3
$Ca_{0.08}Co_4Sb_{12.45}$	−0.78	68	160	316	2.3
$Ca_{0.20}Co_4Sb_{12.47}$	−1.6	99	232	180	1.4

ation of this quantity. The Pauli susceptibility χ_{Pauli} can be written in the form[46]

$$\chi_{Pauli} = \left(\frac{m^*}{m_0} - \frac{1}{3}\frac{m_0}{m^*}\right)\chi_P^{LDA}, \quad (9)$$

where χ_P^{LDA} stands for the paramagnetic term deduced from the LDA calculations using the free-electron formula

$$\chi_P^{LDA}[\text{emu mol}^{-1}] = N\mu_B^2 N(E_F) = 2.376 \times N(E_F), \quad (10)$$

with N the number of electrons per one mole of formula unit, μ_B the Bohr magneton, and $N(E_F)$ the calculated DOS expressed in states/Ry per formula unit. Here the evaluated DOS, in confrontation, e.g., with experimentally determined Sommerfeld coefficient γ (using low-temperature specific heat data) or theoretically calculated value can bring useful information on the character of the charge carriers close to the Fermi level.

Taking into account the difficulties with paramagnetic impurities, we deduced the Pauli susceptibility χ_{Pauli} from $\chi_{intrinsic}$ at room temperature as their role is minimized. As there are no magnetic dopants in the $Ca_xCo_4Sb_{12}$ skutterudites, the only task, however very delicate, in evaluation of the χ_{Pauli} represents the correct subtraction of the lattice susceptibility χ_{latt} [see Eq. (8)]. Let us comment on this point. Supposing a "purely" ionic bonding with spherical electron orbits, one can simply evaluate χ_{latt}^{ionic} by "adding up" the total number of electrons in the formula. For Co_4Sb_{12} this simple assumption leads to $\chi_{latt}^{ionic} \sim -720 \times 10^{-6}$ emu mol^{-1}. However, in the case of compounds with covalent bonding and/or valence electrons with other than s symmetry, this value must be corrected to the orbital contribution reflecting the character of the bonding-orbital occupations and their magnetic spectroscopy. The exact evaluation of this correction, known mostly as Van Vleck paramagnetic component (χ_{latt}^{VV}), is not a simple task and exceeds the frame of this work. So we propose, as the most appropriate approximation, to estimate the correct core susceptibility using the tabulated values for "core" susceptibilities of Sb and Co ions with "closest" bonding characteristics as that in Co_4Sb_{12}. As only available, we have found the susceptibilities for SbH_3 (Ref. 46) and isolated Co^{3+} ions which yields $\chi_{latt}^{covalent} \sim -448 \times 10^{-6}$ emu mol^{-1}. This value, confronted with overestimated "purely ionic" $\chi_{latt}^{ionic} \sim -720 \times 10^{-6}$ emu mol^{-1}, insinuates the "reasonable" value of $\chi_{latt}^{VV} \sim +280 \times 10^{-6}$emu mol^{-1} and thus was used for the evaluation of Pauli's susceptibility.

Using Eq. (9), we can compare the values χ_{LDA} provided by the LDA theoretical calculation and that of experimentally deduced χ_{Pauli} and evaluate the effective mass. As can be seen in Table II, very reasonable values are observed taking into account the fact that the experimental values of χ_{Pauli} are affected by a large uncertainty due to both experimental error and the approximation used in the determination of the lattice susceptibility. Nonetheless, we underline that a very good agreement with values presumed from the literature for n-type Co skutterudites as well as that determined on a base of magnetotransport data (Table I) is observed and confirms independently the enhancement of the high effective mass of the conducting electrons. Moreover, a small value of χ_{Pauli} observed for $x=0$ insinuates the presence of free charge carries. This observation is absolutely consistent with transport data revealing a high carrier density and high electrical conductivity at 300 K. A more detailed analysis of this contribution is, however, doubtful, taking into account the large experimental error and, notably, the presumed low effective mass of holelike carriers, which significantly enhances their Langevin diamagnetism competing with Pauli paramagnetism [see Eq. (9)].

D. Electronic specific heat

As the specific heat, Cp, data can provide useful information about both the charge carrier and the lattice dynamics, we have performed comparative measurements of the specific heat for Ca-free and Ca-rich $x=0.20$ samples. In order to evidence simultaneously the low-temperature electronic contribution and the large effect of the Ca filler above the 15 K, the experimental data of both compounds were compared and are plotted in Fig. 13 in a usual way as $C_p/T = \gamma + \beta T^2$ (γ and β are the electron and phonon contributions, respectively). We see that the difference between the two compounds $x=0$ and $x=0.20$ at low temperatures tends to the Sommerfeld coefficient $\gamma \sim 28$ mJ mol^{-1} K^{-2}, which confirms the existence of the finite DOS at E_F. Here, similarly to the case of the previously discussed Pauli susceptibility, an alternative method to evaluate m^* exists via a comparison of the Sommerfeld coefficient γ with that obtained from LDA band calculations, γ^{LDA}.

Using the $N(E_F)$ obtained by the LDA band calculations, we can deduce the value of the electronic specific heat coef-

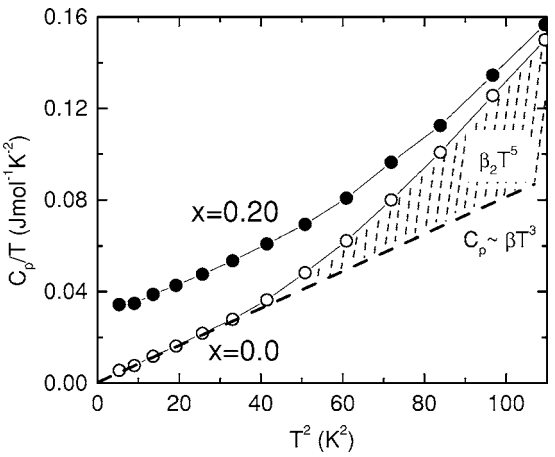

FIG. 13. The low-temperature specific heat for $Ca_{0.20}Co_4Sb_{12}$ (●) and Co_4Sb_{12} (◯). The anharmonic contribution to the specific heat of Co_4Sb_{12} proportional to $\beta_2 T^5$ is evidenced by shaded area above the dashed line.

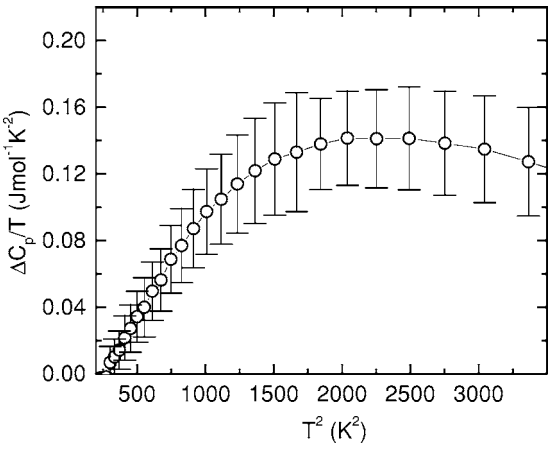

FIG. 14. The difference between $Ca_{0.20}Co_4Sb_{12}$ and Co_4Sb_{12} specific heats plotted up to 60 K.

ficient γ^{LDA} in the noninteracting limit. Applying the simple equation

$$\gamma^{\mathrm{LDA}} = \frac{\pi^2}{3} k_B^2 N(E_F), \tag{11}$$

then

$$\gamma^{\mathrm{LDA}}\ [\mathrm{mJ/(mol\ K^2)}] = 0.173 N(E_F). \tag{12}$$

The KKR-CPA density of states at the Fermi level obtained in Ca-containing skutterudites (Fig. 10) results in the following γ^{LDA} values: 8, 12, and 17 mJ mol^{-1} K^{-2} for $x=0.05$, 0.10, and 0.20, respectively. In the case of $x=0.20$ the theoretical result can be directly compared to the experimental data, which also allows one to estimate the effective mass from the ratio $\gamma/\gamma^{\mathrm{LDA}}=m^*/m_0=1.6$. This value is in surprisingly good agreement with that of experimentally determined on the basis of Pauli susceptibility and thermopower analysis, respectively (Tables I and II). Moreover, the ratio

$$\left(\frac{m^*}{m_0}\right)\chi_{\mathrm{Pauli}} \Big/ \left(\frac{m^*}{m_0}\right)\gamma$$

does not deviate significantly from unity (for $x=0.20$) and points to a classical noninteracting electron system without strong electron correlations the enhancement of which over unity is characteristic for systems with electron correlations.[48] In other words, it is appropriate to assume roughly a one-to-one correspondence between the quasiparticle excitations in $Ca_{0.20}Co_4Sb_{12}$ and those of a free-electron gas.

In order to evidence the large effect of the Ca filler above the 15 K the experimental data of the $CoSb_3$ ($4\times$) were subtracted from that of $Ca_{0.20}Co_4Sb_{12}$ and the difference is plotted in usual way in Fig. 14. The data are, however, burdened by a huge experimental error, understandable considering the experimental uncertainty making the subtraction of the data delicate. Despite this ambiguity, the additive specific heat of $Ca_{0.20}Co_4Sb_{12}$ with respect to $CoSb_3$ is evident and enabled us to perform the fit of the dissipative Einstein mode associated with Ca atoms. The attempt to fit both the Ca concentration and the characteristic temperature yielded reasonable values of the Einstein temperature $\Theta_E \sim 140$ K and concentration $x \sim 0.4 \pm 0.2$, which matches fairly well with chemical analysis providing $x=0.20$. A strong anharmonicity of skutterudite structure lattice dynamics itself is also evident from the low-temperature data of $CoSb_3$ presented in Fig. 13. The typical assumption of the linear $C_p/T=\beta T^2$ dependence is valid only below $T \sim 6$ K when at higher temperatures a reasonable fit supposing $C_p=\beta T^3+\beta_2 T^5$ can be made. Such an approximation provides a relatively high Debye temperature $\Theta_D \sim 380$ K, which is, however, consistent with a strongly covalent character of $CoSb_3$ bonding. The anharmonicity of the lattice dynamics for "pure" $CoSb_3$ was experimentally observed by Feldman *et al.*[49]; however, the data were not explicitly commented on. Nonetheless, the theoretical analysis permits us to explain this unusual feature by the peculiar bonding of antimony where, namely, the intersquare Sb force constants insinuate possible intrinsic anharmonicity.

IV. SUMMARY AND CONCLUSIONS

We have presented comprehensive experimental and theoretical investigations of low-temperature electronic, transport, and magnetic properties in partially filled $Ca_xCo_4Sb_{12}$ skutterudites using electrical resistivity, thermopower, Hall coefficient, susceptibility, and specific heat measurements as well as the KKR-CPA electronic structure calculations.

The thermopower of $Ca_xCo_4Sb_{12}$ is quite large and decreases (in absolute value) regularly with increasing Ca content. The sign of the thermopower is consistent with a negative value of measured R_H. It was found that the change of the Seebeck coefficient slope α/T versus Ca concentration can be tentatively related to the variation of the calculated DOS at the Fermi level.

On the other hand, the electrical conductivity in $Ca_xCo_4Sb_{12}$, being more sensitive to the impurity electronic states, varies in complex way with x concentration. This behavior was attributed to the presence of the large s-DOS peak from Ca at the conduction band. This theoretical result is well supported by measured low value of the Hall carrier

mobility as well as the important value of electron effective mass as derived from the thermopower curves. The carrier scattering mechanism elucidated from the electronic structure features (at least in the range of 5%–10% Ca content) seems to be consistent with the observed Mott-like character of the resistivity curves. The KKR-CPA computations also showed that Ca inserted into the void of $CoSb_3$ behaves as a double-electron donor, which is in line with the experimental carrier concentration detected in $Ca_{0.08}Co_4Sb_{12}$. Conversely, the decrease of the electron concentration observed for $x=0.20$ indicates a different conductivity mechanism that could be attributed to modifications of the Fermi-surface properties (well supported by increasing the hybridization of Ca *s* states with the electronic states of the host material). Moreover, the electronic specific heat measured in $Ca_{0.20}Co_4Sb_{12}$ (with respect to the binary parent $CoSb_3$) favorably fits with the computed DOS value at E_F.

On the whole, the KKR-CPA computations along the alkaline-earth series $A_xCo_4Sb_{12}$ (A=Mg, Ca, Sr, Ba) showed that Ca is a unique case due to the unusual electronic structure. It would be then interesting to compare the low-temperature physical properties of $Ca_xCo_4Sb_{12}$ to those of $Ba_xCo_4Sb_{12}$ and $Sr_xCo_4Sb_{12}$, since the calculations predict more "rigidlike" behavior of the electronic structure in these latter.

ACKNOWLEDGMENT

It is a pleasure to acknowledge useful conversations with L. Chaput regarding this work. The authors thank financial support of PAI Barrande.

*Corresponding author. Electronic address: lenoir@mines.inpl-nancy.fr

[1] C. Uher, in *Semiconductors and Semimetals*, edited by T. Tritt (Academic Press, San Diego, 2000), Vol. 69, p. 139.
[2] G. P. Meisner, Physica B **108**, 763 (1981).
[3] E. Bauer, St. Berger, Ch. Paul, M. Della Mea, G. Hilscher, H. Michor, M. Reissner, W. Steiner, A. Grytsiv, P. Rogl, and E. W. Scheidt, Phys. Rev. B **66**, 214421 (2002).
[4] G. I. Shirotani, T. Uchiumi, K. Ohno, C. Sekine, Y. Nakazawa, K. Kanoda, S. Todo, and T. Yagi, Phys. Rev. B **56**, 7866 (1997).
[5] J. W. Sharp, E. C. Jones, R. K. Williams, P. M. Martin, and B. C. Sales, J. Appl. Phys. **78**, 1013 (1995).
[6] T. Caillat, A. Borshchevsky, and J.-P. Fleurial, J. Appl. Phys. **80**, 4442 (1996).
[7] B. Chen B., J.-H. Xu, C. Uher, D. T. Morelli, G. P. Meisner, J.-P. Fleurial, T. Caillat, and A. Borshchevsky, Phys. Rev. B **55**, 1476 (1997).
[8] D. T. Morelli, G. P. Meisner, B. Chen, S. Hu, and C. Uher, Phys. Rev. B **56**, 7376 (1997).
[9] G. S. Nolas, J. L. Cohn, and G. A. Slack, Phys. Rev. B **58**, 164 (1998).
[10] H. Takizawa, K. Miura, M. Ito, T. Suzuki, and T. Endo, J. Alloys Compd. **282**, 79 (1999).
[11] N. R. Dilley, E. D. Bauer, M. B. Maple, and B. C. Sales, J. Appl. Phys. **88**, 1948 (2000).
[12] G. S. Nolas, M. Kaeser, R. T. Littleton IV, and T. M. Tritt, Appl. Phys. Lett. **77**, 1855 (2000).
[13] B. C. Sales, B. C. Chakoumakos, and D. Mandrus, Phys. Rev. B **61**, 2475 (2000).
[14] G. S. Nolas, H. Takizawa, T. Endo, H. Sellinschegg, and D. C. Johnson, Appl. Phys. Lett. **77**, 52 (2000).
[15] L. D. Chen, T. Kawahara, X. F. Tang, T. Goto, T. Hirai, J. S. Dyck, W. Chen, and C. Uher, J. Appl. Phys. **90**, 1864 (2001).
[16] J. S. Dyck, W. Chen, C. Uher, L. Chen, X. Tang, and T. Hirai, J. Appl. Phys. **91**, 3698 (2002).
[17] X. Tang, Q. Zhang, L. Chen, T Goto, and T. Hirai, J. Appl. Phys. **97**, 093712 (2005).
[18] G. A. Lamberton, Jr., S. Bhattacharya, R. T. Littleton IV, M. A. Kaeser, R. H. Tedstrom, T. M. Tritt, J. Yang, and G. S. Nolas, Appl. Phys. Lett. **80**, 598 (2002).
[19] J. S. Dyck, W. Chen, J. Yang, G. P. Meisner, and C. Uher, Phys. Rev. B **65**, 115204 (2002).
[20] J. Yang, M. G. Endres, and G. P. Meisner, Phys. Rev. B **66**, 014436 (2002).
[21] J. Yang, D. T. Morelli, G. P. Meisner, W. Chen, J. S. Dyck, and C. Uher, Phys. Rev. B **67**, 165207 (2003).
[22] V. L. Kuznetsov, L. A. Kuznetsova, and D. M. Rowe, J. Phys.: Condens. Matter **15**, 5035 (2003).
[23] G. S. Nolas, J. Yang, and H. Takizawa, Appl. Phys. Lett. **84**, 5210 (2004).
[24] M. Puyet, B. Lenoir, A. Dauscher, M. Dehmas, C. Stiewe, and E. Müller, J. Appl. Phys. **95**, 4852 (2004).
[25] M. Puyet, A. Dauscher, B. Lenoir, M. Dehmas, C. Stiewe, E. Müller, and J. Hejtmanek, J. Appl. Phys. **97**, 083712 (2005).
[26] M. Puyet, B. Lenoir, A. Dauscher, P. Weisbecker, and S. J. Clarke, J. Solid State Chem. **177**, 2138 (2004).
[27] G. S. Nolas, M. Kaesar, R. T. Littleton IV, T. M. Tritt, T. H. Sellinschegg, and D. C. Johnson, in *Thermoelectric Materials 2000 - The Next Generation Materials for Small Scale Refrigeration and Power Generation Applications*, edited by T. M. Tritt, G. S. Nolas, G. Mahan, M. G. Kanatzidis, and D. Mandrus, MRS Symposia Proceedings No. 626 (Materials Research Society, Warrendale, PA, 2001).
[28] A. Bansil, S. Kaprzyk, P. E. Mijnarends, and J. Tobola, Phys. Rev. B **60**, 13396 (1999).
[29] T. Stopa, S. Kaprzyk, and J. Tobola, J. Phys.: Condens. Matter **16**, 4921 (2004).
[30] S. Kaprzyk and A. Bansil, Phys. Rev. B **42**, 7358 (1990).
[31] L. Chaput, P. Pecheur, J. Tobola, and H. Scherrer, Phys. Rev. B **72**, 085126 (2005).
[32] J. Yang, G. P. Meisner, D. T. Morelli, and C. Uher, Phys. Rev. B **63**, 014410 (2000).
[33] K. T. Wojciechowski, J. Tobola, and J. Leszczynski, J. Alloys Compd. **361**, 19 (2003).
[34] L. D. Chen, T. Kawahara, X. F. Tang, T. Goto, T. Hirai, J. S. Dyck, W. Chen, and C. Uher, in *Proceedings of the 19th International Conference of Thermoelectrics*, edited by D. M. Rowe (Brabow Press, Cardiff, 2000), p. 348.

[35] K. Matsubara, T. Sakakibara, Y. Notohara, H. Anno, H. Shimizu, and T. Koyanagi, in *Proceeding of the 15th International Conference on Thermoelectrics*, edited by T. Caillet, A. Borshchevsky, and J.-P. Fleurial (IEEE, New York, 1996), p. 96.
[36] M. Puyet, Ph.D. thesis, Institut National Polytechnique de Lorraine, Nancy, 2004.
[37] H. J. Goldsmid, in *Thermoelectric Refrigeration* (Temple Press Books Ltd, London, 1964).
[38] D. J. Singh and W. E. Pickett, Phys. Rev. B **50**, 11235 (1994).
[39] J. O. Sofo and G. D. Mahan, Phys. Rev. B **58**, 15620 (1998).
[40] H. Anno, K. Hatada, H. Shimizu, K. Matsubara, Y. Notohara, T. Sakakibara, H. Tashiro, and K. Motoya, J. Appl. Phys. **83**, 5270 (1998).
[41] N. F. Mott, J. Non-Cryst. Solids **1**, 1 (1968).
[42] X. Shi, L. Chen, J. Yang, and G. P. Meisner, Appl. Phys. Lett. **84**, 2301 (2004).
[43] J. Y. W. Seto, J. Appl. Phys. **46**, 5247 (1975).
[44] I. Lefebvre-Devos, M. Lassalle, X. Wallart, J. Olivier-Fourcade, L. Monconduit, and J. C. Jumas, Phys. Rev. B **63**, 125110 (2001).
[45] K. Koga, K. Akai, K. Oshiro, and M. Matsuura, Phys. Rev. B **71**, 155119 (2005).
[46] S. V. Vonsovskii, in *Magnetism* (John Wiley & Sons, and Keter Publishing House, Jerusalem Ltd, New York, 1974), Vol. 1.
[47] T. Rosenqvist, Acta Metall. **1**, 762 (1953).
[48] K. Wilson, Rev. Mod. Phys. **47**, 773 (1975).
[49] J. L. Feldman, D. J. Singh, I. I. Mazin, D. Mandrus, and B. C. Sales, Phys. Rev. B **61**, R9209 (2000).